

# PILOTED FLIGHT SIMULATION FOR HELICOPTER OPERATION TO THE QUEEN ELIZABETH CLASS AIRCRAFT CARRIERS

Michael F Kelly, Mark D White, Ieuan Owen

School of Engineering  
University of Liverpool  
Liverpool, UK

Steven J Hodge

Flight Simulation  
BAE Systems – Warton Aerodrome  
Preston, UK

## Abstract

Flight simulation is being used to inform the First of Class Flight Trials for the UK's new Queen Elizabeth Class (QEC) aircraft carriers. The carriers will operate with the Lockheed Martin F-35B Lightning II fighter aircraft, i.e. the Advanced Short Take-Off and Vertical Landing variant of the F-35. The rotary wing assets that are expected to operate with QEC include Merlin, Wildcat, Chinook and Apache helicopters. An F-35B flight simulator has been developed and is operated by BAE Systems at Warton Aerodrome. The University of Liverpool is supporting this project by using Computational Fluid Dynamics (CFD) to provide the unsteady air flow field that is required in a realistic flight simulation environment. This paper is concerned with a research project that is being conducted using the University's research simulator, HELIFLIGHT-R, to create a simulation environment for helicopter operations to the QEC. The paper briefly describes how CFD has been used to model the unsteady airflow over the 280m long aircraft carrier and how this is used to create a realistic flight simulation environment. Results are presented from an initial simulation trial in which test pilots have used the HELIFLIGHT-R simulator to conduct simulated helicopter landings to two landing spots on the carrier, one in a disturbed air flow and the other in clean air. As expected, the landing to the spot in disturbed air flow requires a greater pilot workload, shows greater deviation in its positional accuracy and requires more control activity. This initial trial is the first of a planned series of simulated helicopter deck landings for different wind angles and magnitudes.

## 1. INTRODUCTION

The first of the United Kingdom's two new aircraft carriers, HMS Queen Elizabeth, shown in Fig. 1, is currently undergoing sea trials. The construction of the second carrier, the Prince of Wales, is well advanced. At 65,000 tonnes each, with a length of 280m and a beam of 73m, they are the largest warships ever built for the Royal Navy.



Figure 1 HMS Queen Elizabeth aircraft carrier

The Queen Elizabeth Class (QEC) carriers will operate with the highly augmented Advanced Short Take-Off and Vertical Landing (ASTOVL) variant of the Lockheed Martin F-35B Lightning II fighter aircraft [1]. Characteristic features of the QEC, as can be seen in Fig. 1, include the twin island layout, and the ramp, or "ski-jump", at the bow to facilitate short take-off. The concurrent development of the QEC and F-35B programmes has presented a unique opportunity to deploy modelling and simulation to optimise the aircraft-ship interface and maximise the combined capabilities of these two assets [2]. As well as the fixed-wing F-35B, it is expected that the QEC carriers will also operate rotary-wing assets such as Merlin, Wildcat, Chinook and Apache helicopters.

The University of Liverpool (UoL) has been at the forefront of research into the use of modelling and simulation to better understand the air flow environment around a ship's landing deck and how this affects the flying qualities of the aircraft and the workload of the pilot. The disturbed air flow over the ship's superstructure is due to a combination of the ship's forward speed and the prevailing wind, and is known as the ship's 'airwake'. To enable the airwake to be included in the simulation environment, it is modelled using Computational Fluid Dynamics

(CFD). The majority of the research conducted by the UoL has been with single-spot frigates and destroyers, and two principal aims of this ongoing work are (i) to create a flight simulation environment for realistic helicopter launch and recovery operations [3], and (ii) to develop guidance for ship designers to minimise the effect of ship topside aerodynamics on a helicopter [4]; both aims being directed towards maximising operational capability and reducing pilot workload during helicopter launch and recovery operations.

Currently the UoL is working with BAE Systems to apply their expertise to develop a simulation environment for the QEC in the fixed-wing F-35B motion simulator operated by BAE [5]. UoL's contribution is to provide the very large unsteady airwakes for integration into the simulation environment.

Separately, with joint funding from the Engineering and Physical Sciences Research Council and BAE Systems, UoL is creating a simulation environment for the QEC to be implemented in its research simulator HELIFLIGHT-R. This paper describes some of the initial results from this research.

Determining the safety margin and pilot workload for helicopter launch and recovery operations under different conditions takes place during First of Class Flight Trials (FOCFTs), allowing crews to perform a risk assessment according to aircraft payload, sea-state, visibility, and wind speed and direction [6]. FOCFTs are used to determine Ship-Helicopter Operating Limits (SHOL), which thereafter provides a guide to pilots and crew identifying the maximum permissible limits for a given helicopter landing on a given ship deck in a range of wind speeds and directions.

SHOLs are currently determined by the Royal Navy through FOCFTs for each ship-helicopter combination, using test pilots to perform numerous landings in a wide range of conditions at sea. During SHOL testing, limits are determined using the Deck Interface Pilot Effort Scale (DIPES) [7], with a rating being awarded by a test pilot for each attempted landing based on the workload experienced and an assessment of whether or not an average fleet pilot could consistently repeat the landings safely. Flight test engineers also interpret aircraft power and control margins to inform the DIPES rating.

Once the pilot ratings have been awarded for each wind speed, direction, and sea-state the completed wind envelope for a given ship-helicopter combination can be produced. The SHOL diagram illustrates the safe boundaries for each wind speed and direction at a specified Corrected All Up Mass (CAUM). Maximum permissible deck motion angles are also listed in the SHOL diagram [6].

The FOCFT process, while reliable, carries numerous practical difficulties and incurs considerable expense, with crews and equipment engaged for several weeks in the task of determining a SHOL for each new ship-helicopter combination. Even after several weeks at sea the desired environmental conditions might not be encountered, with crews relying upon the forecast of wind and sea-state conditions to be within reach of the ship to complete testing. Indeed, aircraft mass is often the only fully controllable variable during SHOL testing.

With increasing defence budget constraints facing many nations, a more cost-effective method of producing SHOLs for future ship-helicopter combinations is desirable. Simulation of the aircraft-ship Dynamic Interface (DI) may present a cost-effective aid to real-world SHOL testing, with continuing improvements in simulation fidelity making this option increasingly feasible.

Flight simulation facilities at UoL include the HELIFLIGHT-R flight simulator, which has a six degrees of freedom motion platform and a visual scene with a wide field of view; the simulator has been successfully used in several previous simulation research projects, e.g. [3, 4, 8]. Internal and external views of the HELIFLIGHT-R flight simulator are shown in Fig. 2.



**Figure 2** QEC visual environment in the HELIFLIGHT-R flight simulator

Simulation of the ship-aircraft DI requires effective modelling of an aircraft's flight dynamics, unsteady ship airwakes, and ship motion. Realistic visual models are also required, including sea surface, ship geometry, deck markings, and visual landing aids.

Previous ship airwake research at UoL has been carried out for single-spot (i.e. frigate-size) ships; the QEC aircraft carriers are significantly larger multi-spot platforms, with a requirement to operate both fixed-wing and rotary-wing aircraft. The increased size and complexity of the QEC airwakes requires a new approach to ensure the computed CFD has the

required fidelity for flight simulation. This paper first describes some of the computational challenges and the experimental validation required to ensure confidence in the CFD airwakes, before describing some results of simulated deck landings.

## 2. AIRWAKE MODELLING

To create a high fidelity simulation, a validated set of CFD airwakes has been incorporated into the flight simulators at UoL and BAE Systems Warton to recreate the effects of unsteady air flow in the proximity of the landing areas and downwind of the ship. ANSYS Fluent was selected as the CFD solver, employing the Delayed Detached Eddy Simulation (DDES) SST  $k-\omega$  based turbulence model with third-order accuracy. This use of Large Eddy Simulation (LES) in the domain free-shear flow region offers the twin advantages of time-accurate resolution of Reynolds stresses, and reduced dissipation due to eddy viscosity when compared with a “pure” Unsteady Reynolds-Averaged Navier-Stokes (URANS) approach [9].

The increased computational demands of the larger airwakes required by an aircraft carrier model have necessitated a different CFD approach to that used on smaller frigate-size ships [10]. The increased size of the QEC immediately increases computational expense to maintain sufficient cell density in the region of the 280m×70m flight-deck. Additionally, and more significantly, the primary requirement for the aircraft carrier CFD airwake is to accurately maintain the airwake unsteadiness along the fixed-wing approach path to the ship, where the aircraft can begin to experience the airwake of the carrier at up to half a mile prior to landing [11]. The QEC CFD airwake will also be required to accommodate Vertical Landing (VL) approaches of fixed- and rotary-wing aircraft, further increasing the mesh cell count required. Previous work by the US Naval Air Systems Command (NAVAIR) has produced 7 million cell CFD grids for the 333-metre-long Nimitz class USS George Washington (CVN-73) [12], however initial efforts found this grid density to be insufficient for a DDES study on this scale, with a 120 million cell mesh required to resolve turbulence both along the Shipborne Rolling Vertical Landing (SRVL) glideslope [13], and around the six VL spots on the flight deck.

Preparing the ship geometry for CFD requires decisions to be made about the appropriate simplifications that can be applied to the geometry. The surface cell size that has been adopted is 30cm, with 12 prism layers grown from this surface mesh. Geometry features are prepared accordingly, requiring user experience to determine where mesh problems are likely to occur. In the generation of a very large mesh, which must be carried out using High-Performance Computing (HPC), each step of

mesh generation can be computationally intensive, with mesh problems difficult to rectify using a desktop computer.

### 2.1. Boundary Conditions

The ship geometry was placed in a cylindrical domain of 4.5 ship lengths radius (1260m) and a height of 0.75 ship lengths (210m), providing sufficient distance to prevent far field interference in the vicinity of the ship and glideslope focus regions. A cylindrical domain was used so that different wind directions can be obtained by simply adjusting the inlet x and y velocity components. All surfaces of the aircraft carrier were modelled as zero-slip walls. The upper surface of the domain was set as a pressure-far-field, permitting flow to move vertically out of the domain, and thus minimising any potential for blockage. The sea surface was set as a wall with a slip condition, thereby allowing a prescribed inlet velocity profile to be maintained throughout the domain. The inlet velocity into the domain was modelled to reproduce the Earth’s Atmospheric Boundary Layer (ABL) at sea using Eqn. (1), where:  $V_{ref}$  is the reference wind-speed measured at a known height above sea-level,  $Z_{ref}$ , and  $Z_0$  is the sea-surface roughness length scale which, according to [14], can be taken to equal 0.001m for oceanic conditions.

$$V = V_{ref} \left( \frac{\ln \left( \frac{Z}{Z_0} \right)}{\ln \left( \frac{Z_{ref}}{Z_0} \right)} \right) \quad (1)$$

The reference wind speed is the vector sum of the ship speed and true wind speed at anemometer height, with the ABL profile adjusted accordingly for any combination of ship speed, wind speed, and wind azimuth.

### 2.2. Glideslope Turbulence

A significant challenge for CFD modelling of the aircraft carrier airwake is to accurately represent the turbulence in the velocity components along the fixed-wing glideslope due to the unsteady wake of the ship, through which the aircraft must pass during a landing. In aircraft carrier operations, this massively separated unsteady airwake region off the stern and in the lee of the carrier is known as the “carrier burble” [15]. To accurately resolve the carrier burble, the mesh must be refined locally, resulting in a significant increase in cell count. The nominal QEC approach paths for SRVL and VL are illustrated in Fig. 3. Without a burble cell density region, the QEC mesh will be of the order of 30 million cells. With the burble density region included, the cell count increases to roughly 120 million cells to capture the flow detail up to 0.25 miles aft of the ship.

The interpolation boxes in Fig. 3 refer to the reduced volume of the CFD domain that is implemented in the

simulator; both the larger fixed-wing interpolation box and the smaller helicopter interpolation box are shown, along with the much smaller interpolation box used for previous studies relating to frigates [3]. The larger box, which is implemented in the BAE F-35B simulator, is 700m long, 200m wide and 72 m high. The smaller box, which is implemented in HELIFLIGHT-R, is 300m by 150m by 24m.

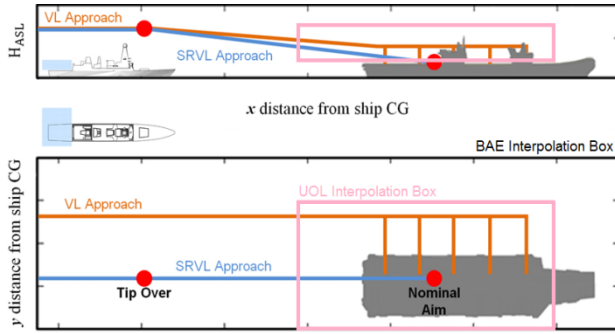


**Figure 3** Interpolation box sizing for UoL and BAE simulators, compared with previous interpolation box size used for frigates and destroyers at UoL

### 2.3. Simulation Settling Time

The flight simulation requires a 30 second airwake, which is then looped in the simulation software; however, prior to reaching the desired 30 second sampling time, the CFD calculations must first be permitted to settle to ensure a repeatable solution. An increased ship length results in an increased CFD simulation settling time. As an unsteady solution begins, the fluid should pass over the length of the ship several times for the flow to acquire a fully unsteady state. For a 130m long frigate at a wind speed of 40kts, it will take approximately 15 seconds for the flow to pass over the ship 2.5 times. For a 280m long aircraft carrier at 25kts, it will take approximately 60 seconds for the flow to begin to achieve a settled transient solution, requiring several hours of CPU time per second of CFD simulation. The free-stream velocity can be increased to reduce settling time, provided flow remains incompressible; however, it is important that the Courant-Friedrichs-Lewy (CFL) condition is obeyed across the ship, requiring a compromise between settling time and time-step in the simulation set-up [16].

In practice, numerous sampling points were placed throughout the domain, and were monitored until the mean velocity in three components was seen to converge. From this experience, Eqn. (2) has been adopted as a useful approximation of the simulation settling period, where  $t_{set}$  is the settling time,  $L$  is the characteristic length over which the fluid will pass, and  $V$  is the free-stream velocity.

$$t_{set} \approx \frac{2.5L}{V} \quad (2)$$

It should be noted that this settling time is used as a rule-of-thumb only, with actual settling time varying in practice due to a range of factors (e.g. time-step, iterations per time-step, mesh quality, boundary conditions). The total wall-clock time required per run was found to be approximately 30 days using 128 processors, depending upon settling behaviour for a given wind strength and direction.

### 2.4. Post-processing Data

Data file size for the larger fixed-wing QEC CFD simulation has also to be taken into consideration. Raw data files (containing full simulation data) are approximately 3.5TB per wind-direction. Manipulation of this data presents challenges and cannot easily be achieved using desktop computers. Instead, HPC must be used for data processing, placing increased demands upon shared resources. Data storage and transfer also presents challenges, with even the fastest Solid State Drives reading/writing at 550/520MB/s.

Upon completion of a CFD simulation for a given wind direction, the airwake velocity data must then be converted into a format which can be integrated into the flight simulator. The unstructured data is first interpolated onto a structured grid in the region of interest (the interpolation box), as illustrated earlier in Fig. 3, before being output in ASCII format. Examples of an unstructured and structured grid can be seen in Fig. 4. The output ASCII airwake data can then be imported into the simulator's flight dynamics modelling software, where verification takes place to ensure that the airwake is correctly positioned relative to the ship's visual model in the flight simulation environment.

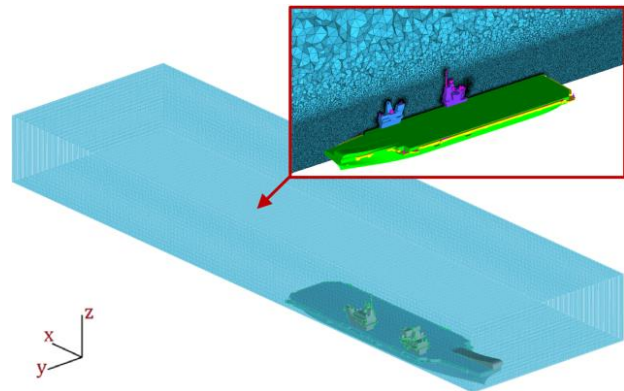


**Figure 4** QEC unstructured CFD exported as a set of structured air-wake look-up tables

### 2.5. Experimental Validation of Airwakes

As mentioned earlier, previous airwake research at UoL has concentrated on frigate size ships with CFD-generated airwakes being compared with wind tunnel and with at-sea measurements [10]. The QEC airwakes are clearly much larger and so an

experimental programme is being conducted to provide measured data for comparison with CFD. The details of the experimental programme and the results obtained thus far are outside of the scope of this paper, but, in brief, a 1:200 scale model of QEC has been manufactured and has been immersed in a water tunnel where three-component velocity measurements have been made using an Acoustic Doppler Velocimeter (ADV). A brief introduction to the experimental facility and some measurements along the SRVL glide path have been presented in [17], but a more comprehensive study will be reported in due course. In summary, the experimental measurements are showing good agreement with the CFD results.

## 2.6. QEC Airwake

Figure 5 shows the ship's airwake in a headwind, represented by contours of the mean horizontal velocity component in a vertical plane through the centre of the islands (bottom) and another through the centreline of the ramp (top). Also shown is the velocity profile of the ABL, described by Eqn. (1). The reference velocity ( $V_{ref}$ ) is at the anemometer height ( $z_{ref}$ ) of 34m above mean sea level. As expected, in a headwind, the islands create significant wakes while the flow over the ramp and the flight deck is relatively undisturbed. To get a better idea of the locations of the two vertical planes in Fig. 5, the reader is referred to Figs. 1 and 7. Some additional CFD output is provided later in the Results section.

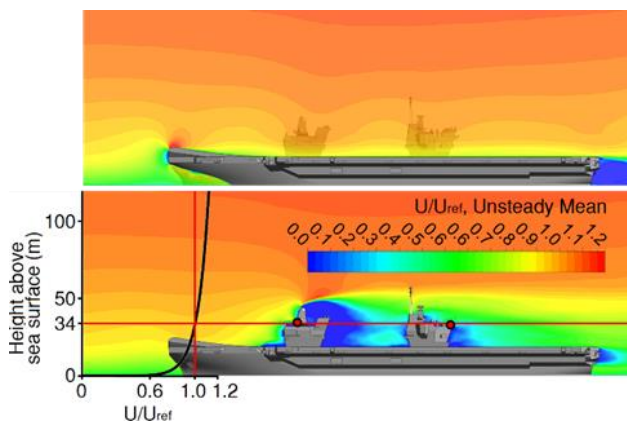


**Figure 5** QEC aircraft carrier airwake including ABL. Vertical planes through centrelines of islands (bottom), and ramp (top).

## 3. HELICOPTER FLIGHT SIMULATION

The HELIFLIGHT-R flight simulator, shown earlier in Fig. 2, is capable of motion in six axes, employing six actuators each with a 24-inch stroke. Motion base acceleration commands are provided as outputs from the aircraft flight dynamics model, which are passed through a motion drive algorithm. A fully programmable control loading system provides force-feedback through the aircraft cyclic, collective, and

pedal inceptors. Integration of the aircraft flight dynamics model with the simulator is achieved using Advanced Rotorcraft Technology's (ART's) FLIGHTLAB software [18], which provides a library of aircraft models, including a generic rotorcraft flight model that has been re-configured at UoL to be representative of the Sikorsky SH-60B Seahawk used in this trial. Although the Seahawk is not in use with the Royal Navy, it was decided that this aircraft model would be used for these proof-of-concept simulation trials due to its strong validation and extensive previous use at Liverpool [3,4]. CFD airwakes can be integrated with FLIGHTLAB, enabling unsteady airwake velocities to be imposed upon the aircraft flight model. During testing, FLIGHTLAB allows real-time data monitoring and recording which, together with in-cockpit video and audio recordings, are used for post-trial analysis.

As well as the helicopter flight dynamics model and the airwake, the simulator also needs to present the pilot with a realistic visual environment that not only provides appropriate visual cues but is also consistent with the location of the airwake. In this initial trial, ship motion was not applied (i.e. no deck roll, pitch or heave) other than there being a wind over deck.

### 3.1. Integrating the Airwake with FLIGHTLAB

The purpose of the initial simulated flight trial reported in this paper was to demonstrate capability of the QEC dynamic interface simulation for helicopter launch and recovery, and so it was decided that the landings would be performed for three wind-speeds – 25kts, 36kts, and 45kts, at one wind direction – Ahead. The CFD solution was computed for a headwind at 36kts. The 100Hz computations were then sampled at 25Hz, and interpolated onto a structured grid that corresponds with the UoL interpolation box shown earlier in Fig. 3 for helicopter flight tests. This airwake was then scaled using FLIGHTLAB to obtain 25kts and 45kts conditions for the same WOD. The methodology and validation of this scaling technique has been demonstrated by Scott et al. [19].

The integration process is described schematically in Fig. 6. The unsteady velocity components ( $u, v, w$ ) in the three-dimensional domain ( $x, y, z$ ) are reduced in volume from the original unstructured cylindrical domain at 100Hz into the orthogonal structured grid of the interpolation box at 25Hz. The reduced data is then imported into FLIGHTLAB as look-up tables. The velocity components are applied to the helicopter flight model at Aerodynamic Computation Points (ACPs) on the helicopter. The positions of the ACPs on the SH-60B model can be seen in the upper-right of Fig. 6, with ten ACPs on each of the four main rotor blades, one at the fuselage, one on each of the port

and starboard stabilisers, two on the vertical tail, and a final ACP at the centre of the tail rotor hub, to give a total of 46 ACPs.

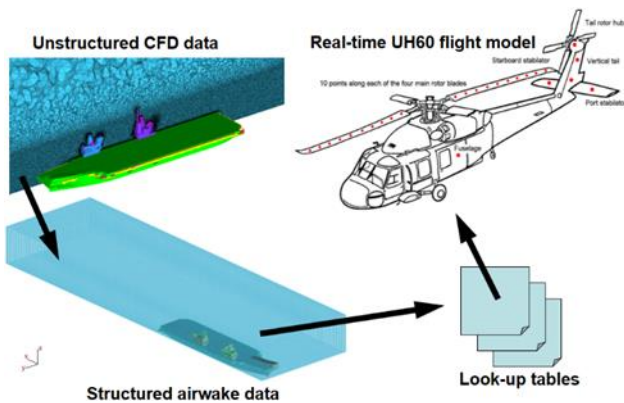


**Figure 6** Integration of CFD airwake with helicopter flight dynamics model

To ensure the velocity field, defined by the reformatted, down-sampled and transposed airwake, was still applying the correct velocity components to the ACPs in the flight model, a series of checks were made to confirm that the unsteady velocities in the original airwake were consistent with those experienced at the ACPs.

### 3.2. Flight Trials

Once the QEC visual scene, airwake, and SH-60B Seahawk flight dynamics model had been successfully integrated and tested in the HELIFLIGHT-R flight simulator, a series of piloted flight tests were conducted.

For flight testing to QEC in the Ahead case, landings were performed to Spot 5 (port) and Spot 6 (starboard), as it is anticipated that these will be the primary landing spots for helicopters. The locations of these spots towards the stern of the ship can be seen in Fig. 7. In the headwind case, a helicopter landing to Spot 5 can be expected to be in relatively clean air, while it will be in disturbed air in lee of the islands when landing to Spot 6.

For Spot 5, landings were performed by following the standard Royal Navy port-side forward-facing recovery technique, typically employed when landing on single-spot frigates and destroyers and illustrated to the left in Fig. 7. For Spot 6 however, a port-side approach was not appropriate since the aircraft would have to traverse across Spot 5 prior to landing, which is undesirable if an aircraft is stationed at that spot. While an approach from the starboard side was considered feasible, landings to Spot 6 during the flight trial were performed using an approach from the stern. The stern approach is shown on the right side of Fig. 7.

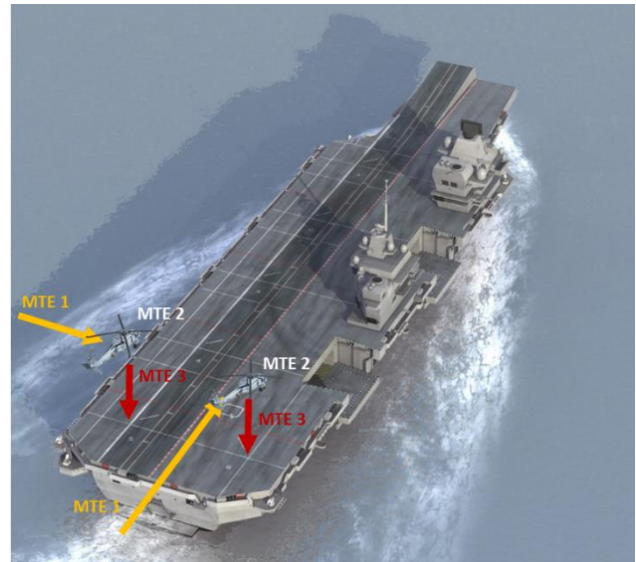


**Figure 7** Port-side forward-facing approach to spot 5 and stern approach to spot 6. Landing tasks each divided into 3 MTEs

The landing procedure was split into three Mission Task Elements (MTEs), with each MTE shown in Fig. 7. Starting from a position one rotor diameter off the deck edge, MTE 1 consists of a translation across the flight-deck stabilising at a position above the landing spot, at a hover height of 30ft, in preparation to land. MTE 2 consists of a 30 second period of hover station-keeping prior to the landing. Finally, MTE 3 is the descent from the hover position to touchdown on the flight-deck. A spatial tolerance of  $\pm 3.5$  metres in all three directions was selected as the desirable positional accuracy during the hover station-keeping task.

Flight simulator testing was performed with the assistance of two highly experienced former Royal Navy test pilots over a period of four days. The landing task was performed at three headwind speeds (25kts, 35kts, and 45kts) at both landing spots (5 and 6) by both pilots. This gave a total of 12 separate landing attempts, which was achievable in the time available with the test pilots.

During the flight trial, upon completion of each MTE, the test pilot was asked to provide a subjective rating using the Bedford workload rating scale. The Bedford workload rating scale is a 10-point scale used by evaluation pilots to assess the workload required to successfully complete a given task. Ratings 1-3 are awarded when the workload is considered to be satisfactory without reduction and does not prevent the pilot from performing additional tasks (e.g. monitoring systems or radio communications). Ratings of 4-6 are awarded where the workload for an MTE is deemed to be tolerable, while a rating of 7-9 is awarded where the task can be performed successfully, yet the workload is not tolerable for the

task. Finally, a rating of 10 is awarded in situations where the pilot is unable to complete the MTE, and so must abandon the task. A more complete description of the Bedford workload rating scale and its use in flight simulation can be found in [3].

Once the pilot had completed each mission (i.e. a full landing to the QEC deck), in addition to Bedford workload ratings for each of the three MTEs, the pilot was also required to award a DIPES rating for the overall difficulty of the landing. The DIPES scale requires the test pilot to give a rating of 1-5 for any given launch/recovery task. A rating of 1-3 is considered to be acceptable, with the task considered to be within the abilities of an average fleet pilot. Conversely, a rating of 4 is deemed to be unacceptable on the basis that an average fleet pilot would not be able to complete the task in a consistently safe manner, while a rating of 5 indicates that the task cannot be safely completed by the test pilot even under controlled test conditions. Additionally, the test pilot can apply one or more letter suffixes to a DIPES rating which describe the cause(s) of the increased workload (e.g. T for turbulence). The DIPES ratings scale is widely used amongst NATO member countries in the determination of SHOL envelopes for a given ship-aircraft combination. Again, a more complete description of the DIPES scale and its application to simulated deck landings can be found in [3].

In addition to Bedford and DIPES ratings and pilot comments, simulation flight test data was also recorded for each MTE. This test data is used to better understand the quantitative and qualitative feedback provided by the pilot, providing time-domain recordings of aircraft position, attitude, velocities, and accelerations in six axes. Cyclic, collective, and pedal positions are also recorded, in addition to air-wake velocity components at ACPs.

### 3.3. Results

In the headwind, the landing spot requiring the largest pilot workload was found to be Spot 6, as expected, because of the highly turbulent flow shedding from the ship's islands. Landings at Spot 5 were found to be more benign with lower levels of variance in instantaneous velocity magnitude and direction found over Spot 5. The difference in air flow turbulence intensity over the two spots is shown clearly in Fig. 8.

Bedford workload ratings for each MTE and DIPES ratings for each complete Landing mission are given in Table 1; the aerodynamic causes of these ratings are discussed below, together with an assessment of pilot control activity and aircraft responses due to these disturbances. It is noticeable that the two pilots have awarded different ratings on the 10 point Bedford scale; this represents their subjective experience of the test points flown and, whilst there

are numerical differences, the variations in the ratings are typical of piloted trials.

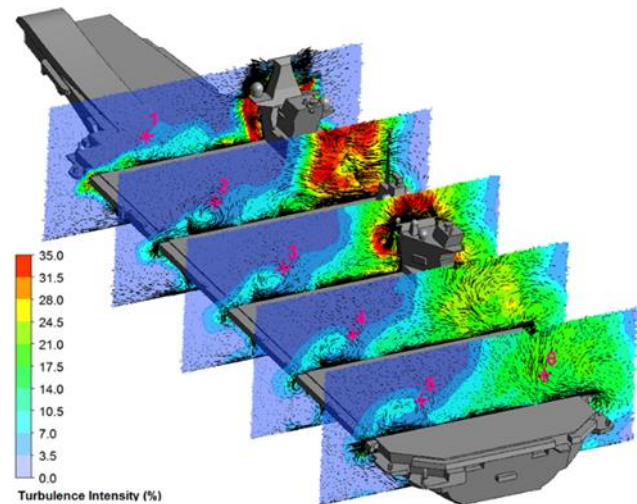


**Figure 8** Mean turbulence contours and velocity vectors in transverse planes through QEC landing spots 1-6

**Table 1** Bedford & DIPES ratings for Spots 5 & 6, Ahead case

			MTE 1	MTE 2	MTE 3	DIPES
PILOT 1	Spot 5	25kts	3	3	3	1
		35kts	3	3	4	1
		45kts	4	4	4	1
	Spot 6	25kts	3	4	4	1
		35kts	4	5	5	1
		45kts	5	7	6	2
PILOT 2	Spot 5	25kts	2	2	2	1
		35kts	2	2	2	1
		45kts	2	2	3	1
	Spot 6	25kts	3	3	3	1
		35kts	3	3	3	1
		45kts	3	5	6	3

As can be seen, higher wind speed over deck does not necessarily correlate with increased pilot workload. For example, while it can be seen that workload will tend to increase with wind speed over Spot 6 where disturbed air is encountered, Spot 5 overall showed a lower correlation between wind speed and pilot workload. This is because the pilot performing a landing to Spot 5 will experience mostly undisturbed airflow, and thus will not have a higher workload as the airspeed increases provided the landing can be performed within the control limits of the aircraft.

#### 3.3.1. Results for Spot 5

During flight testing, landings to Spot 5 were rated as having a consistently lower workload than Spot 6 at all wind speeds, on both the DIPES and Bedford workload rating scales, and for both test pilots. Both pilots also held the aircraft well within the spatial limits of  $\pm 3.5$  metres set for the hover task, as can be seen

in Fig. 9, where the orange boxes represent these set limits at the height of the aircraft centre of gravity for a 30ft hover. This comparatively low workload is largely due to the lower levels of disturbed air passing over the aircraft at this position, as can clearly be seen in the airwake data in Fig 8, with the only ship geometry upstream of Spot 5 being the ski-jump, positioned 200m away towards the bow.

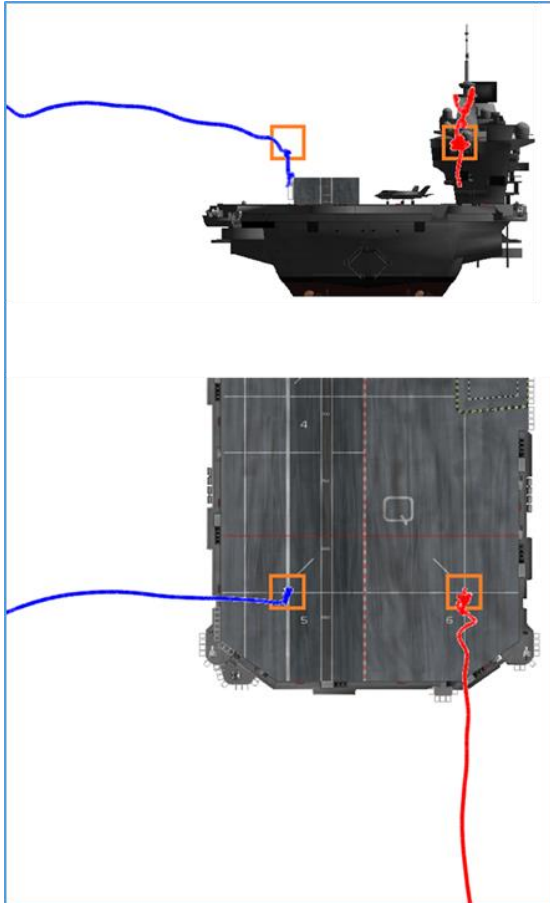


**Figure 9** Locus of SH-60 centre of gravity on approach to QEC; Pilot 2, Spots 5 & 6, Ahead 45kts

During the landing task (MTE3) to spot 5, both pilots reported experiencing a disturbance just prior to touchdown at approximately six metres above the flight deck; Pilot 1 reported “*small corrections [were] required on the way down*” for Spot 5 at 35kts, while Pilot 2 reported “*a small lateral disturbance*” for Spot 5 at 45kts. The lateral disturbance experienced by Pilot 2 six metres above deck can just be seen in Fig. 9 where, during MTE3 for Spot 5 (blue), the aircraft can be seen to move laterally to starboard, requiring the pilot to pause the descent briefly while making corrections.

The reason for these small disturbances when descending to Spot 5 can be seen in Fig.8 where there is a small area of turbulent air close to the spot (albeit much less than over Spot 6). The source of this turbulence can be traced to the bow of the ship and

the ski-jump ramp. Figure 10 shows, through mean streamlines, that a vortex is formed in the headwind condition and passes along the deck parallel to Spots 1-5 (the locations of which can be seen on Fig. 8), with the vortex core approximately 5 metres to port of the landing spots, and 5 metres above the flight deck. Figure 10 shows how the vortex is formed by flow passing along the chamfer on the port underside of the ski-jump, to then be channelled along the forward port-side catwalk and onto the flight deck. This turbulent flow then forms a three-dimensional vortex which “*corkscrews*” along the port edge of the ski-jump and along landing spots 1-5.

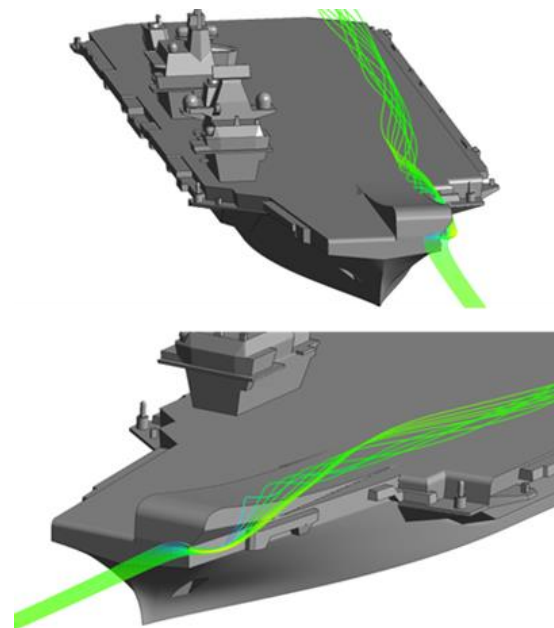


**Figure 10** Vortex passing along landing spots 1-5, originating from ski-jump & forward port catwalk

### 3.3.2. Results for Spot 6

Compared with Spot 5, Bedford workload and DIPES ratings were consistently higher for Spot 6, as listed in Table 1. The increased pilot workload is a result of the highly unsteady wake shedding from the islands upstream of the landing spot, as seen in Fig. 8. Further, as a stern approach was used for the approach to Spot 6, both pilots experienced disturbances to the aircraft throughout MTE1, with Pilot 2 stating “*airwake [is] obvious from the moment [MTE1] started*” for Spot 6 at 45kts; this is significant given that at the beginning of MTE1, the aircraft was positioned 53 metres behind the stern of the ship.

In addition to the increased workload ratings reported by both pilots, control input magnitudes could be seen to be increased in comparison with Spot 5, reflecting the increased corrections required to compensate for the increased disturbances on the aircraft. Throughout the manoeuvres to Spot 6 it was also reported that while “*aircraft disturbances [were felt] in all axes*”, the dominant axis was felt by the pilots to



be the pitch axis during station-keeping at MTE2. Analysis of the aircraft control inputs support this observation by the test pilots, and is shown in Fig. 11, with lateral and longitudinal stick inputs plotted for each WOD to Spot 5 (blue, left) and Spot 6 (red, right).

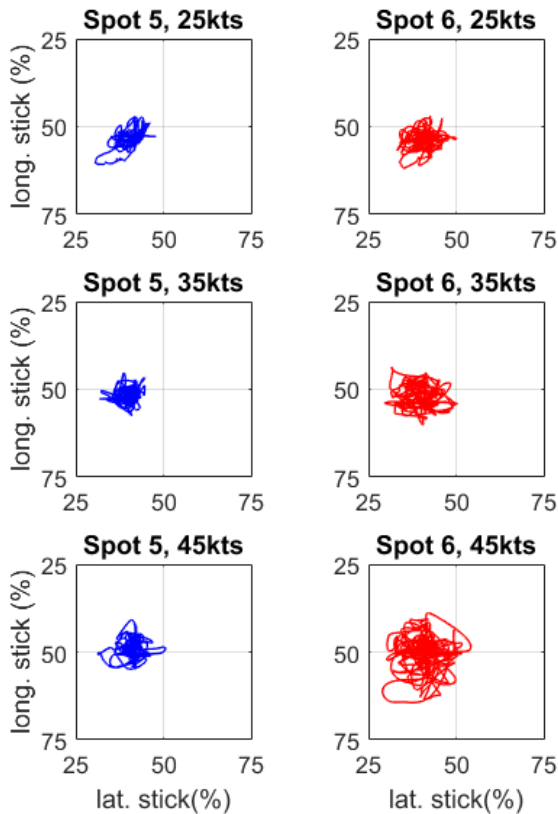


**Figure 11** Pilot 2 cyclic control inputs for MTE 2 & 3 at Spot 5 & Spot 6

It is clear from Fig. 11 that the range of stick control inputs required to maintain a stabilised hover is greater for Spot 6 compared to Spot 5, as would be expected for operation in a more turbulent region of the ship. Spot 6 came within 28% of the maximum lateral control limit in the 45kts condition, and within 30% of the lateral control limit at 35kts, with remaining control percentages greater than 10% considered to be acceptable during testing, suggesting remaining stick control was not a limiting factor in the awarding of DIPES ratings.

The collective and pedal control inputs are shown as percentages of total available control in Fig. 12 for Spot 5 (blue), and Spot 6 (red). Each MTE is indicated on the diagram, allowing a better understanding of variation in pilot control inputs between tasks. General comparison of collective inputs in Fig. 12 shows an increased standard deviation between Spot 5 and Spot 6 of 5.7% and 4.7% respectively, with collective control input range of 35.3 – 46.7% for Spot 5, and 30.6 – 51.1% for Spot 6. This increased variance in collective input was due to increased

disturbance of the aircraft in heave during approach and hover for a landing to Spot 6, and was reported by Pilot 1 as “light ballooning” during MTE1 at 25kts, with Pilot 2 commenting “[I] felt vertical bumps during the mission”.

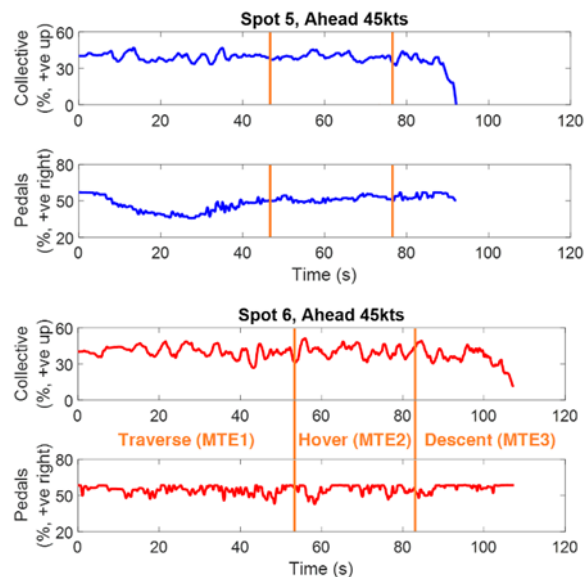


**Figure 12** Pilot 2 collective & pedal inputs for Spot 5 (blue), and Spot 6 (red), for 3 MTEs in Ahead 45kts.

Comparison of pedal control input percentages between the two spots, Fig. 12, shows overall increased use of the left pedal during MTE1 for landings to Spot 5 compared with Spot 6, with this input required to maintain heading during traverse across the ship, as would be expected. This is due to the increased lateral relative wind speed passing over the tail rotor during the traverse in MTE1 (and ‘weathercock’ action of the fuselage), resulting in a change of angle of attack on the tail rotor, altering the torque and required corrective pedal input from the pilot. For this reason, maximum deviation of pedal controls from the trim condition occurred over Spot 5 during MTE1, however with minimum 35% control remaining in the left pedal, yaw was not considered a significant control axis during the Ahead landings. During MTE2 it can be seen from Fig. 12 that, while pedal inputs are generally steady during the hover over Spot 5, regular left pedal inputs are required when hovering over Spot 6 to maintain heading; this is due to the vertical aircraft disturbances noted by the pilots and the required cross-coupled pilot response to maintain plan position. At 45kts, the pedal input range was 35.7 – 57.1% for Spot 5, and 43.0 – 58.6% for Spot 6, while standard deviation from pedal trim point for Spot 5 was 1.9%, while at Spot 6 this was doubled to 3.8%. As the minimum remaining pedal control margin was at least 35.7% during testing in the Ahead 45kts case to Spots 5-6, it can be concluded that pedal control limits were not critical to the DIPES rating, and so the yaw control axis was not significant during landings in the Ahead case.

However, it should be noted when traversing across the deck during approach from the port-side in a Green WOD, pedal limits are likely to be more critical to the mission.

#### 4. CONCLUDING COMMENTS

This paper has described how a research flight simulation environment has been developed for the QEC aircraft carriers. Airwakes have been created using CFD and, although not presented in this paper, experimental validation is currently underway and is showing good agreement with the CFD. The very large airwake domains, due to the size of the ship and of the glide path used by the fixed-wing F-35B aircraft, are very demanding of computational resources and computing time.

The airwakes have been implemented in the BAE F-35B simulator and, as described in this paper, in the UoL HELIFLIGHT-R simulator.

Initial flight trials have been conducted in both simulators and some results for helicopter landings to the QEC have been presented for a headwind. Two landing spots on the ship were selected; one with disturbed air, being in the lee of the islands, and the other in relatively clean air.

The flight trials have demonstrated the increased difficulty of landing in the disturbed air flow in the lee of the islands with higher pilot workload ratings, increased control inceptor activity and reduced positional accuracy. The unsteady aerodynamic loads experienced by the helicopter and the pilot are consistent with, and can be explained by, the CFD-generated unsteady air flow.

Due to the twin-island configuration of the QEC, it can be expected that the aerodynamic influences on aircraft launch and recovery will vary significantly with wind direction and strength; simulated flight trials under oblique wind conditions are ongoing.

#### References

1. Bevilaqua, P.M. "Inventing the F-35 Joint Strike Fighter", 47<sup>th</sup> AIAA Aerospace Sciences Meeting Including the New Horizons Forum and Aerospace Exposition, Orlando, Florida. AIAA 2009-1650, January 2009.
2. Lison, A. "Integrating the Joint Combat Aircraft into the Queen Elizabeth Class Aircraft Carriers – Design Challenge or Opportunity?", Warship 2009 – 'Airpower at Sea', London, UK, June 2009.
3. Hodge, S.J., Forrest, S.J., Padfield, G.D. & Owen, I. "Simulating the environment at the aircraft-ship dynamic interface: research, development, & application". The Aeronautical Journal, November 2012, Vol. 116, No. 1185, pp. 1155-1184.
4. Forrest, J.S., Kääriä, C.H. & Owen, "Evaluating ship superstructure aerodynamics for maritime helicopter operations through CFD and flight simulation". The Aeronautical Journal, October 2016, Vol. 120, No. 1232, pp.1578-1603.
5. Hodge S.J., & Wilson P.N. "Operating JSF from CVF: The reality of simulation". In Proceedings of the International Powered Lift Conference, RAeS, London, 22-24 July 2008.
6. Carico, G.D., Fang, R., Finch, R.S., Geyer Jr, W.P., Krijins, H.W. & Long, K. "Helicopter/Ship Qualification Testing". NATO SCI-055 Task Group, RTO-AG-300 Vol 22, February 2003.
7. Finlay, B.A., "Ship Helicopter Operating Limit Testing – Past, Present and Future", RAeS Rotorcraft Group Conference on Helicopter Operations in the Maritime Environment, London, UK, March 2001.
8. White, M.D., Perfect, P., Padfield, G.D., Gubbels, A.W. & Berryman, A.C. "Acceptance testing and commissioning of a flight simulator for rotorcraft simulation fidelity research". Proceedings of the IMechE, Part G: Journal of Aerospace Engineering, April 2013, Vol. 227, Iss. 4, pp. 663–686.
9. Spalart, P.R., Deck, S., Shur, M.L., Squires, K.D., Strelets, M. Kh. & Travin, A. "A New Version of Detached-Eddy Simulation, Resistant to Ambiguous Grid Densities". Theoretical and Computational Fluid Dynamics, 2006, Vol. 20, Iss 3, pp. 181-195.
10. Forrest, J.S. & Owen, I. "An investigation of ship airwakes using Detached-Eddy Simulation". Computers & Fluids, 2010, Vol. 39, pp. 656-673.
11. Rudowsky, T. et al., "Review of the Carrier Approach Criteria for Carrier-Based Aircraft – Phase I; Final". Patuxent River, MD: Naval Air Warfare Center Aircraft Division, Rept. NAWCADPAX/TR-2002/71, October 2002.
12. Polsky, S. & Naylor, S. "CVN Airwake Modeling and Integration: Initial Steps in the Creation and Implementation of a Virtual Burble for F-18 Carrier Landing Simulations". AIAA Modeling and Simulation Technologies Conference and Exhibit, San Francisco, California, August 2005.
13. Cook, R. et al., "Development of the Shipborne Rolling Vertical Landing (SRVL) Manoeuvre for the F-35B Aircraft". International Powered Lift Conference, October 2010.

14. Garratt, R. "The atmospheric boundary layer". Cambridge Atmospheric and Space Science Series, Cambridge University Press, 1992.
15. Kelly, M.F., White, M.D., Owen, I. & Hodge, S.J. "Using airwake simulation to inform flight trials for the Queen Elizabeth Class Carrier", IMarEST 13<sup>th</sup> International Naval Engineering Conference and Exhibition (INEC 2016), Bristol UK, April 2016.
16. Anderson, J.D. "Computational fluid dynamics: the basics with applications". McGraw-Hill, 1995.
17. Kelly, M.F., White, M.D., Owen, I. & Hodge, S.J. "The Queen Elizabeth Class Aircraft Carriers: Airwake Modelling and Validation for ASTOVL Flight Simulation", American Society of Naval Engineers Launch & Recovery Symposium, MITAGS, Linthicum Heights, MD USA, Nov 16-17 2016.
18. Duval, R.W. "A real-time multi-body dynamics architecture for rotorcraft simulation," in RAeS Proceedings of the challenge of realistic rotorcraft simulation, London, UK, 7-8 November, 2001.
19. Scott, P., White, M.D. & Owen, I. "The effect of ship size on airwake aerodynamics and maritime helicopter operations", 41<sup>st</sup> European Rotorcraft Forum, Munich, 1-4 September 2014.